

Forces and torques on spheroidal particles in various types of viscous shear flow

By **PIERO OLLA**

ISIATa-CNR, Polo Scientifico Universitá di Lecce, 73100 Lecce Italy

(Received 2 December 2024)

The behavior of rigid spheroidal particles in a viscous flow is analysed using a vector spherical harmonics representation of the Stokes equation. This representation allows to clearly separate flow components associated with force, torque and stress. At the same time, it is possible to catalog forces and torques on particles in shear flows, in function of particle shape and shear characteristics, in a very simple way. Various applications have been discussed. The transverse displacement of a spheroidal particle due to the encounter with another particle in a linear shear has been calculated. The corresponding contribution to shear induced transverse diffusivity in suspensions has been obtained as well. The torque on a not fore-aft symmetric particle in a channel flow, has been calculated, and the relevance of this effect to the migration of particles to the middle of narrow ducts has been discussed.

1. Introduction

The dynamics of suspensions is determined by the flow modifications, produced by the particles in the fluid. If interest is focused on volumes small enough for viscosity to be dominant, the perturbed fluid flow will adjust itself instantaneously to the varying boundary conditions. In this picture, the fluid plays only an auxiliary role, furnishing the medium for particle-particle, particle-mean flow and particle-solid obstacle effective interactions. If, furthermore, the suspension is not too concentrated, the perturbation in the fluid flow, will be obtained, to a first approximation, by linear superposition of the individual contributions by the different particles. These approximations stand at the basis of most modelling of suspension dynamics.

The simplest suspension model, in which the particles are rigid and spherical, and the flow is purely viscous, unfortunately, does not account for important physical processes, such as the transverse displacement of particles, due to two-particle encounters, or particle interactions with solid obstacles. This leads to under-estimate the amount of transverse particle diffusivity and migration in sheared suspensions.

The role of inertia in causing transverse migration, in the presence of external forces (Saffman 1965), or of walls bounding the flow (Ho & Leal 1974, Vasseur & Cox 1976), has been studied over the years (see McLaughlin 1993 for recent references). Only recently, however, has similar interest been directed to understanding how a non-spherical shape affects the behavior of a particle in suspension. Felderhof and Jones (1994a,b) considered the problem of how a micro-organism is able to swim thanks to periodic deformations of its body; the drift of ellipsoidal particles has been studied in the context of sedimentation in Russel *et Al.* (1977) and, more recently in Olla (1997a,b) and Olla (1998), to understand the dynamics of red cells in the vicinity of a blood vessel wall.

The velocity disturbance produced around a non-spherical particle is very difficult to

calculate, and with a few exceptions, such as the ellipsoid in a linear shear (see e.g. Jeffery 1922), no analytical solutions exist. For shapes close to spherical, however, perturbation theory becomes possible and analysis of the modification to the particle dynamics produced by different kinds of deviation from sphericity and of external flow, can be carried on. In this way, qualitative informations can be obtained, on the way certain crude aspects of the particle shape (e.g. the amount of fore-aft asymmetry) and of the external flow (e.g. linear or quadratic shear) affect the particle dynamics.

Decomposition of the velocity field and of the deviation from sphericity, respectively, in vector and scalar spherical harmonics, is a powerful tool used first in Felderhof & Jones (1994b) and later in Olla (1997a), to carry on perturbation theory in Stokes flows. Using vector spherical harmonics leads in fact, to a very compact representation of velocity and pressure perturbations, which becomes especially helpful when using symbolic manipulation programs such as Maple. Purpose of this paper is to present in ordered form various expressions of practical use in calculations, such as vector spherical harmonics decompositions for pressure, velocity and stress for flows in internal and external domains. At same time, several applications, such as calculation of forces and torques on spheroidal particles, and modifications to their trajectories, will be illustrated, side by side with geometrical proofs extending some of the results beyond perturbation theory.

This paper is organized as follows. In section II the basis of the formalism are developed, giving expression for velocity, pressure, vorticity and radial stresses, in terms of vector spherical harmonics. In section III, using this formalism, a simple technique for the calculation of forces and torques, around spheroidal particles in arbitrary flow fields, is developed. In section IV, this technique is used explicitly to show that only certain deviations from spherical shapes, lead to forces and torques on spheroidal particles in a linear strain flow. In section V, the modifications to particle trajectories, produced by deviation from spherical shape, in large cross section binary particle encounters, are examined. The contribution to shear induced transverse diffusion is calculated, showing that, in the dilute limit, diffusivity in a suspension of non-spherical particles must be linear in the concentration. In section VI, the torque on a particle with no fore-aft symmetry, placed in a quadratic shear, is calculated, and the relevance of the process to the transverse migration of particles in narrow channels is analysed. Section VII is devoted to discussion of the results and to concluding remarks. The appendix contains various considerations on the possibility that individual particles follow chaotic trajectories, thus contributing to suspension diffusivity.

2. Stokes equation in vector spherical harmonics

In a perturbative analysis around a spherically symmetric situation, it is convenient to expand the velocity field in terms of vector spherical harmonics $\mathbf{Y}_{lm}^\mu(\hat{x}_i)$, $\mu = s, l, m$:

$$\mathbf{v}(\mathbf{x}) = \sum_{lm} [v_{lm}^s(x) \mathbf{Y}_{lm}^s(\hat{x}_i) + v_{lm}^e(x) \mathbf{Y}_{lm}^e(\hat{x}_i) + v_{lm}^m(x) \mathbf{Y}_{lm}^m(\hat{x}_i)], \quad (2.1)$$

where $\hat{x}_i = x_i/x$ are the cosines of \mathbf{x} in an appropriate reference frame and the superscripts {sem}, standing for scalar, electric and magnetic, come from the origin of this basis as a tool in the study of electromagnetic waves (see Landau & Lifshitz 1982). In terms of standard spherical harmonics the functions $\mathbf{Y}_{lm}^\mu \equiv |\mu| l m$ are defined as

$$\mathbf{Y}_{lm}^s(\hat{x}_i) = \hat{\mathbf{x}} Y_{lm}(\hat{x}_i) \quad \mathbf{Y}_{lm}^e(\hat{x}_i) = \frac{x \nabla Y_{lm}(\hat{x}_i)}{\sqrt{l(l+1)}} \quad \mathbf{Y}_{lm}^m(\hat{x}_i) = \frac{[\mathbf{x} \times \nabla] Y_{lm}(\hat{x}_i)}{\sqrt{l(l+1)}}, \quad (2.2)$$

where $\hat{\mathbf{x}} = x^{-1}\mathbf{x}$. With this definition (which differs from the one adopted in Olla 1997a), these functions are normalized to one: $\langle \mu' l' m' | \mu l m \rangle = \int d\Omega_x \mathbf{Y}_{l'm'}^{\mu'*}(\hat{x}_i) \cdot \mathbf{Y}_{lm}^{\mu}(\hat{x}_i) = \delta_{\mu\mu'} \delta_{ll'} \delta_{mm'}$, with $d\Omega_x$ solid angle differential around \mathbf{x} .

At stationarity, an incompressible fluid in creeping flow conditions, obeys Stokes equation:

$$\mu \nabla^2 \mathbf{v} = \nabla P \quad (2.3)$$

with μ and P the fluid dynamic viscosity and pressure. Putting together with the continuity equation:

$$\nabla \cdot \mathbf{v} = 0, \quad (2.4)$$

one has the vorticity equation:

$$\nabla^2 [\nabla \times \mathbf{v}] = 0. \quad (2.5)$$

In terms of v_{lm}^{sem} components, the vorticity takes the form:

$$\omega = [\nabla \times \mathbf{v}] = \sum_{\mu l m} \omega_{lm}^{\mu} \mathbf{Y}_{lm}^{\mu} =$$

$$= \frac{1}{x} \sum_{lm} \left(-\sqrt{l(l+1)} v_{lm}^{\text{m}} \mathbf{Y}_{lm}^{\text{s}} - \frac{dx v_{lm}^{\text{m}}}{dx} \mathbf{Y}_{lm}^{\text{e}} + \left(-v_{lm}^{\text{s}} + \frac{1}{\sqrt{l(l+1)}} \frac{dx v_{lm}^{\text{e}}}{dx} \right) \mathbf{Y}_{lm}^{\text{m}} \right) \quad (2.6)$$

and the vorticity equation will read:

$$\left(\frac{d^2}{dx^2} + \frac{2}{x} \frac{d}{dx} - \frac{l(l+1)}{x^2} \right) f_{lm}^{(1,2)} \quad (2.7)$$

with $f_{lm}^{(1)} = \omega_{lm}^{\text{m}}$ and $f^{(2)} = v_{lm}$. The continuity equation takes instead the form:

$$\frac{dv_{lm}^{\text{s}}}{dx} + 2v_{lm}^{\text{s}} - \sqrt{l(l+1)} v_{lm}^{\text{e}} = 0 \quad (2.8)$$

From Eqns. (2.6-8), one obtains the "outside" and "inside" solutions:

$$\begin{cases} v_{lm}^{\text{s}} = a_{lm} x^{-l} + b_{lm} x^{-2-l}, \\ v_{lm}^{\text{e}} = \frac{2-l}{\sqrt{l(l+1)}} a_{lm} x^{-l} - \sqrt{\frac{l}{l+1}} b_{lm} x^{-2-l}, \\ v_{lm}^{\text{m}} = c_{lm} x^{-1-l}; \end{cases} \quad (2.9a)$$

and:

$$\begin{cases} v_{lm}^{\text{s}} = a'_{lm} x^{l+1} + b'_{lm} x^{l-1}, \\ v_{lm}^{\text{e}} = \frac{l+3}{\sqrt{l(l+1)}} a'_{lm} x^{l+1} + \sqrt{\frac{l+1}{l}} b'_{lm} x^{l-1}, \\ v_{lm}^{\text{m}} = c'_{lm} x^l. \end{cases} \quad (2.9b)$$

Substituting back into the Stokes equation, one obtains for the pressure field, respectively in an external and internal domain:

$$P = \mu \sum_{lm} \frac{4l-2}{l+1} a_{lm} x^{-l-1} Y_{lm} \quad \text{and} \quad P = \mu \sum_{lm} \frac{4l+6}{l} a'_{lm} x^l Y_{lm}. \quad (2.10)$$

Similarly, substituting into Eqn. (2.6), one finds for the vorticity; in an external domain:

$$\omega = \frac{1}{x} \sum_{lm} \left(-\sqrt{l(l+1)} c_{lm} x^{-1-l} \mathbf{Y}_{lm}^{\text{s}} + l c_{lm} x^{-1-l} \mathbf{Y}_{lm}^{\text{e}} - \frac{4l+2}{l(l+1)} a_{lm} x^{-l} \mathbf{Y}_{lm}^{\text{m}} \right); \quad (2.11a)$$

in the internal domain:

$$\omega = \frac{1}{x} \sum_{lm} \left(-\sqrt{l(l+1)} c'_{lm} x^l \mathbf{Y}_{lm}^s - (l+1) c'_{lm} x^l \mathbf{Y}_{lm}^e + \frac{4l+6}{l(l+1)} a'_{lm} x^{l+1} \mathbf{Y}_{lm}^m \right). \quad (2.11b)$$

The velocity field is thus partitioned into contributions from the pressure (the a_{lm} terms), and into purely potential flow (the b_{lm} terms) and pressure free, vortical contributions (the c_{lm} terms). It is to be noticed that this is a consequence of the symmetry of the Stokes equation; to make an example, in a representation based on the use of ellipsoidal, rather than spherical harmonics (Lamb 1932, Jeffery 1922), such a separation between different contributions would be lost.

The force density $\mathbf{f}(\mathbf{x})$ on a fluid element at position \mathbf{x} is expressed as the divergence of the stress tensor $S_{ij} = -P\delta_{ij} + \sigma_{ij}$: $\mathbf{f} = \nabla \cdot \mathbf{S}$, where $\sigma_{ij} = \mu(\partial_i v_j + \partial_j v_i)$ is the viscous stress. The force density on an element of a spherical surface bounding the domain is $f_i = \pm x^{-1} x^j S_{ij}$ (positive sign in the case of external domain). Using the relation: $\mathbf{x} \cdot \sigma = \mathbf{x} \cdot \nabla \mathbf{v} + x^i \nabla v_i = (x \partial_x - 1)\mathbf{v} + (x \nabla + \hat{\mathbf{x}})v_x$ (summation over repeated indices assumed), Eqns. (2.9a-b) can be used to calculate the force exerted by the fluid on these surfaces. In the two cases of an external and an internal domain, one finds, respectively:

$$\begin{aligned} \mathbf{f} = \mu \sum_{lm} & \left(-2 \left(\frac{l^2 + 3l - 1}{l+1} a_{lm} x^{-l-1} + (l+2) b_{lm} x^{-l-3} \right) \mathbf{Y}_{lm}^s \right. \\ & + 2 \left((l-1) \sqrt{\frac{l+1}{l}} a_{lm} x^{-l-1} + (l+2) \sqrt{\frac{l}{l+1}} b_{lm} x^{-l-3} \right) \mathbf{Y}_{lm}^e \\ & \left. - (l+2) \sqrt{l(l+1)} c_{lm} x^{-l-2} \mathbf{Y}_{lm}^m \right) \end{aligned} \quad (2.12a)$$

and

$$\begin{aligned} \mathbf{f} = -\mu \sum_{lm} & \left(2 \left(\frac{l^2 - l - 3}{l} a'_{lm} x^l + (l-1) b'_{lm} x^{l-2} \right) \mathbf{Y}_{lm}^s \right. \\ & + 2 \left((l+2) \sqrt{\frac{l}{l+1}} a'_{lm} x^l + (l-1) \sqrt{\frac{l+1}{l}} b'_{lm} x^{l-2} \right) \mathbf{Y}_{lm}^e \\ & \left. + (l-1) \sqrt{l(l+1)} c'_{lm} x^{l-1} \mathbf{Y}_{lm}^m \right) \end{aligned} \quad (2.12b)$$

which is going to be useful e.g. in the calculation of particle deformations from stresses at the particle surface.

3. Representation of forces and torques on particles

If one is interested in the fluid velocity around a particle, the external flow will be decomposed in terms of the "inside" solutions, and the perturbation produced by the particle, in terms of the "outside" ones, which decay at infinity. The force \mathbf{F} on this particle will be calculated integrating the force density on the surface of a sphere enclosing the particle itself and using Eqns. (2.12a-b). It turns out that only the $a_{1m} \mathbf{Y}_{lm}^s$ contributes to the integral. In fact, this is the only term in the sum, which has the right dependence on the distance to produce a momentum flux from infinity to the particle.

$$F_1 = 2\mu\sqrt{6\pi} Re a_{11}; \quad F_2 = -2\mu\sqrt{6\pi} Im a_{11}; \quad F_3 = -2\mu\sqrt{3\pi} a_{10}, \quad (3.1)$$

Now, the coefficients a_{1m} can be expressed in bra-ket notation as: $a_{11} = \frac{x}{2}\{\langle s11| + \sqrt{2}\langle e11|\}|\mathbf{v}\rangle$ and similar for $m \neq 1$. Thus, the force on the particle can be obtained calculating the component of the perturbed velocity on adequate basis functions, which are combinations of "scalar" and "electric" spherical harmonics, and which have the expression:

$$|F_1\rangle = \mu x[-3/2, 0, 0]; \quad |F_2\rangle = \mu x[0, -3/2, 0]; \quad |F_3\rangle = \mu x[0, 0, -3/2]; \quad (3.2)$$

The torque \mathbf{T} can be calculated in a similar way, starting from the expression $T_i = \int d\Omega_x \epsilon_{ijk} x_j f_k x^2 = \int d\Omega_x \epsilon_{ijk} x_j x_l \sigma_{lk}$. Using the expression for the viscous stress $\sigma_{ij} = \mu(\partial_i v_j + \partial_j v_i)$ into the expression for T , leads, after a few manipulations, to the equation:

$$\mathbf{T} = \mu x \int d\Omega_x \{[\mathbf{x} \times \nabla](\mathbf{x} \cdot \mathbf{v}) + [\mathbf{x} \times (\mathbf{x} \cdot \nabla)\mathbf{v}] - [\mathbf{x} \times \mathbf{v}]\}. \quad (3.3)$$

Expanding the velocity field in vector spherical harmonics, one obtains the result that only the v_{1m}^m components contribute to \mathbf{T} :

$$\mathbf{T} = -\frac{\mu\nu}{\sqrt{2}} x^5 \sum_m (v_{1m}^m/x)' \int d\Omega_x \nabla Y_{1m}. \quad (3.4)$$

Notice that, being the velocity a vector and \mathbf{Y}_{lm}^m a pseudo-vector, the coefficient c_{lm} , from Eqn. (2.1), is necessarily a pseudo-scalar. Hence, from Eqn. (3.4), the torque is a pseudo-vector (as it should be) and the c_{1m} component is the only one with the right dependence on the distance, to be associated with an angular momentum flux from infinity to the particle.

Using the expressions for v_{lm}^m provided by Eqn. (2.12a), one obtains the result:

$$T_1 = -4\sqrt{3\pi}\mu R c_{11}; \quad T_2 = 4\sqrt{3\pi}\mu I m c_{11}; \quad T_3 = 2\sqrt{6\pi}\mu c_{10} \quad (3.5)$$

In a way analogous to the case of the force, the torque can be calculated extracting the appropriate components of the velocity field. The associated basis functions are proportional to "magnetic" harmonics with $l = 1$:

$$|T_1\rangle = 3\mu x[0, x_3, -x_2]; \quad |T_2\rangle = 3\rho\nu x[x_3, 0, -x_1]; \quad |T_3\rangle = 3\mu x[x_2, -x_1, 0]. \quad (3.6)$$

It is interesting to notice that Eqns. (3.3) and (3.6), allow to calculate forces and torques on spherical particles without need to calculate the velocity perturbations that are produced in the flow. This formalism provides a technique alternative to the one recently presented in Stone & Samuel (1996), to calculate forces on spherical micro-organisms whose external membranes move in an arbitrary way. In fact, calculating the brackets associated with force and torque on the membrane, one can write: $F_i = \langle F_i | \mathbf{v} \rangle = \langle F_i | \mathbf{v}_B - \bar{\mathbf{v}} \rangle$ and similar for the torque, where \mathbf{v}_B is the membrane velocity and $\bar{\mathbf{v}}$ is the external flow.

As an example, the drag force and torque acting on a rigid, radius r spherical particle, carrying on respectively a translational and a rotational motion, can readily be calculated. In the case of a translation with velocity U , one finds from Eqn. (3.2):

$$F_i = \langle F_i | v \rangle = \langle F_i | U \rangle = -(3/2)\mu r U \int d\Omega_x = -6\pi\mu r U, \quad (3.7)$$

which is the standard Stokes formula for the drag (Batchelor 1967). In the rotation case, take the angular velocity directed along x_3 , with magnitude ω . The velocity at the particle surface is then $\mathbf{v} = \omega[-x_2, x_1, 0]$ and the drag will be:

$$T_3 = \langle T_3 | v \rangle = -3\omega\mu r^3 \int dz d\phi (1 - z^2) = -\frac{8\pi}{3} r^3 \mu \omega. \quad (3.8)$$

As a more interesting example, it is possible to calculate the velocity of a spherical particle at the centre of a quadratic shear flow: $\bar{\mathbf{v}} = \kappa x^2 \mathbf{e}_3$. From Eqn. (3.2), the force is $F_3 = \langle F_3 | \bar{v} \rangle = \mu \kappa r^3 2\pi \int_{-1}^1 dz z^2 = 2\mu \pi \kappa r^3$. Using the expression for Stokes drag, one obtains therefore, that the particle will move with a velocity

$$\mathbf{U} = (6\pi\mu r)^{-1} \mathbf{F} = \frac{\kappa r^2}{3} \mathbf{e}_3. \quad (3.9)$$

Clearly, a much greater effort would have been required if calculation of the velocity perturbation had been required [see e.g. Eqns. (6.3) and (6.5) in section VI].

4. The behavior of a non-spherical particle in a linear strain flow

Consider a fixed quasi-spherical particle in a linear strain flow $\bar{\mathbf{v}} = \kappa(x_2 \mathbf{e}_3 + x_3 \mathbf{e}_2)$. If the particle were spherical, because of the symmetry of the flow, neither forces nor torques would be present on the particle. It is interesting to ask what is the dependence of these forces and torques on the deviation from sphericity. One can describe the particle shape giving the distance of the surface points from the particle centre of mass, taken at the origin of the coordinate system. This quantity $X(\hat{x}_i)$ can be expanded in spherical harmonics:

$$X(\hat{x}_i) = \sum_{lm} X_{lm} Y_{lm}(\hat{x}_i) \quad (4.1)$$

with X_{lm}/r ($r \equiv X_{00}$) a small quantity for $l \neq 0$. The modification to the velocity field produced by the presence of the particle can then be calculated perturbatively in X_{lm}/r . Imposing no-slip boundary conditions on the surface of the spheroid, will produce a contribution \mathbf{v} to the velocity field such that:

$$\mathbf{v}(\mathbf{X}(\hat{x}_i)) = -\bar{\mathbf{v}}(\mathbf{X}(\hat{x}_i)), \quad \mathbf{v}(\infty) = 0 \quad (4.2)$$

and expanding up to first order in X_{lm}/R :

$$\begin{cases} \mathbf{v}^{(0)}(\mathbf{r}) = -\bar{\mathbf{v}}(\mathbf{r}) \\ \mathbf{v}^{(1)}(\mathbf{r}) = -(X(\hat{x}_i) - r) \partial_r (\mathbf{v}^{(0)}(\mathbf{r}) + \bar{\mathbf{v}}(\mathbf{r})) \end{cases} \quad (4.3)$$

where $\mathbf{r} = \hat{\mathbf{x}}r$ and $\mathbf{X} = \hat{\mathbf{x}}X$. The order zero solution is the velocity perturbation around a sphere, whose expression is well known (Batchelor 1967):

$$\mathbf{v}^{(0)}(\mathbf{x}) = 5 \left(\frac{r^5}{x^4} - \frac{r^3}{x^2} \right) \frac{\kappa x_2 x_3 \mathbf{x}}{x^3} - \frac{r^5}{x^5} \kappa [0, x_3, x_2]. \quad (4.4)$$

From Eqns. (3.2) and (3.6), the force and torque on the particle are given by the velocity components: $\langle F_i | \mathbf{v}^{(1)} \rangle$ and $\langle T_i | \mathbf{v}^{(1)} \rangle$, and can be written as:

$$F_i = \mu \kappa \sum_{lm} R_{ilm}^F X_{lm} \quad \text{and} \quad T_i = \mu \kappa r \sum_{lm} R_{ilm}^T X_{lm}. \quad (4.5)$$

The matrix elements R_{ilm}^α , $\alpha = F, T$ have the form:

$$R_{ilm}^\alpha = \int d\Omega_x Y_{lm} R_i^\alpha \quad (4.6)$$

with R_i^α the sum over components of the bras $\langle F_i |$ and $\langle T_i |$ ad those of the velocity gradient $-\partial_r (\mathbf{v}^{(0)}(\mathbf{r}) + \bar{\mathbf{v}}(\mathbf{r}))$, with all terms μ , κ and r factored out. Substituting Eqn. (4.4) and \bar{v} into this gradient and using Eqns. (3.2) and (3.6) for the $|F_i\rangle$ and $|T_i\rangle$, one

obtains the expressions:

$$R_1^F = \frac{9}{2} \frac{x_1 x_2 x_3}{x^3}; \quad R_2^F = \frac{9}{2} \frac{x_2^2 x_3}{x^3} - \frac{15}{2} \frac{x_3}{x}; \quad R_3^F = -\frac{9}{2} \frac{x_2 x_3^2}{x^3} + \frac{15}{2} \frac{x_2}{x} \quad (4.7)$$

and

$$R_1^T = 15 \frac{x_3^2 - x_2^2}{x^2}; \quad R_2^T = 15 \frac{x_1 x_2}{x^2}; \quad R_3^T = 15 \frac{x_1 x_3}{x^2} \quad (4.8)$$

Thus, the only non-zero contributions to R_{ilm}^F are for $l = 1$ and $l = 3$, while R_{ilm}^T receives contribution only from $l = 2$. Now, the $l = 1$ part of $X(\hat{x}_i)$ gives just a displacement of the centre of mass with respect to the origin, with no deviation from spherical shape; thus, only $l = 2$ and $l = 3$ components of X are relevant for the production of force and torque on a particle in linear strain.

Calculating the integral in Eqn. (4.6), one finds the following non-zero contributions to R_{ilm}^F :

$$R_{230}^F = -\frac{9}{5} \sqrt{\frac{\pi}{7}}; \quad R_{331}^F = R_{33-1}^F = i \frac{6}{5} \sqrt{\frac{3\pi}{7}} \\ R_{132}^F = -R_{13-2}^F = 3i \sqrt{\frac{3\pi}{70}}; \quad R_{232}^F = R_{23-2}^F = -3 \sqrt{\frac{3\pi}{70}} \quad (4.9)$$

and:

$$R_{120}^T = 6\sqrt{5\pi}; \quad R_{122}^T = R_{12-2}^T = \sqrt{30\pi} \\ R_{222}^T = -R_{22-2}^T = i\sqrt{30\pi}; \quad R_{321}^T = -R_{32-1}^T = -\sqrt{30\pi} \quad (4.10)$$

It is of particular interest to calculate the dependence on orientation, of the force and torque on a particle in a shear flow. In order to do this, it is necessary to express the deviations from sphericity in the particle and in the laboratory frame, one in the function of the other. Distinguishing with a prime, quantities in the particle reference frame, one can write:

$$X_{lm} = \sum_{m'} d_{mm'}^{(l)} X'_{lm'} \quad (4.11)$$

where the matrix elements $d_{mm'}^{(l)}$ can be expressed in terms of Jacobi polynomials (Landau & Lifshitz 1965, Abramowitz & Stegun 1965) and are given by:

$$d_{mm'}^{(l)} = \int d\Omega_x Y_{lm}^*(\hat{x}_i) Y_{lm'}(\hat{x}'_i) \quad (4.12)$$

As an example, the case of an axisymmetric particle, with its axis lying in the $x_2 x_3$ plane, can be examined more closely. In this case, taking the x'_3 direction along the symmetry axis of the particle, only the $m' = 0$ component of $d_{mm'}^{(l)}$ must be taken into consideration and the primed reference frame is obtained from the laboratory one simply by a rotation around the x_1 axis (see Fig. 1).

The $d_{mm'}^{(l)}$ components are listed below; for $l = 2$:

$$\left\{ \begin{array}{l} d_{00}^{(2)} = -\frac{1}{2} + \frac{3}{2} \cos(\theta) \\ d_{10}^{(2)} = d_{-10}^{(2)} = \frac{i\sqrt{6}}{4} \sin \theta \cos \theta \\ d_{20}^{(2)} = d_{-20}^{(2)} = \frac{\sqrt{6}}{4} \sin^2 \theta \end{array} \right. \quad (4.13)$$

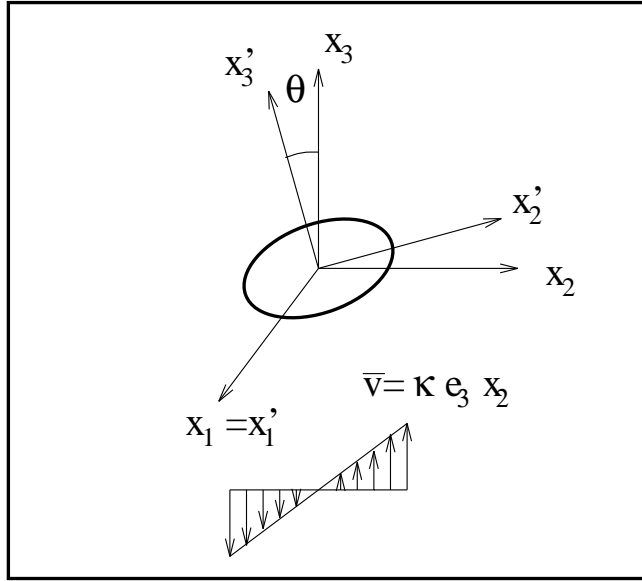


FIGURE 1. Primed and unprimed reference frames. The primed reference frame rotates with the particle with angular velocity $\dot{\theta} = \kappa/2$

while for $l = 3$:

$$\begin{cases} d_{00}^{(3)} = \frac{1}{2} \cos \theta (5 \cos^2 \theta - 3) \\ d_{10}^{(3)} = d_{-10}^{(3)} = \frac{i\sqrt{3}}{4} \sin \theta (5 \cos^2 \theta - 1) \\ d_{20}^{(3)} = d_{-20}^{(3)} = -\frac{\sqrt{30}}{4} \cos \theta \sin^2 \theta \\ d_{30}^{(3)} = d_{-30}^{(3)} = -\frac{i\sqrt{5}}{4} \sin \theta \cos^2 \theta \end{cases} \quad (4.14)$$

Combining Eqns. (4.10) and (4.13), one finds that the torque on an ellipsoidal particle is: $T_1 = 6\sqrt{5}\pi\mu\kappa r^2 X'_{20} \cos 2\theta$, leading, from Eqn. (3.8), to an angular velocity $\omega = \frac{3}{8\pi r^3 \mu} T_1 = \frac{9}{4} \sqrt{\frac{5}{\pi}} \frac{X'_{20}}{r} \cos 2\theta$. Of course, $\omega = a + \cos 2\theta$ is the form of Jeffery's solution to the problem of an ellipsoid in a linear shear (Jeffery 1922). A graphical proof that this is necessarily the functional form for the angular velocity of an axisymmetric ellipsoid in a linear shear is shown in Fig. 2.

An axisymmetric, $l = 3$ deviation for sphericity in a particle means that this has essentially an egg shape, with a concave side if the deviation is large. In Fig. 3, one can see two examples of forces acting on such a particle, when its symmetry axis is parallel to x_3 and to x_2 respectively. In the first case, X_{30} is the only non zero component and from Eqn. (4.9), the force on the particle is directed along x_2 . In the second one, $X_{3\pm 1}$ are the non-zero components of X and in this case the force is along x_3 .

Of course in a linear shear, the vorticity component of the flow would make the particle rotate, so that the end result would be an oscillatory motion of its centre of mass. A steady translation could result however, in the case the particle were able to change its shape in a time dependent manner, in such a way that its axis of symmetry had a privileged orientation, as it may happen in micro-organisms. This could provide an additional propulsion mechanism for such microscopic objects, which would receive part of the energy (depending on the work necessary for deforming their structure) directly from the gradients in the flow field.

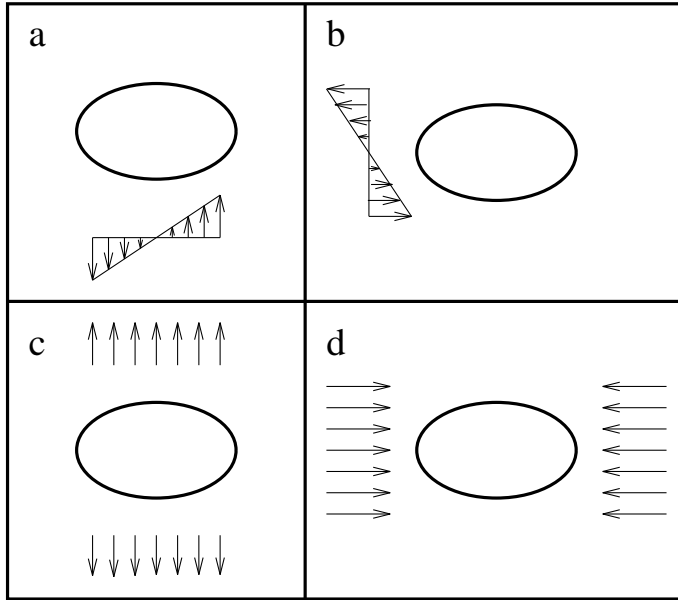


FIGURE 2. Derivation of the functional form for the torque on a fore-aft symmetric particle in linear shear. The flow fields drawn in quadrants (a-d) correspond to the four terms, in the decomposition of the linear shear in the primed reference frame: $\kappa^{-1}\bar{\mathbf{v}} = x_2\mathbf{e}_3 = \mathbf{e}'_3x'_2 \cos^2 \theta - \mathbf{e}'_2x'_3 \sin^2 \theta - \mathbf{e}'_3x'_3 \sin \theta \cos \theta + \mathbf{e}'_2x'_2 \sin \theta \cos \theta$. Flows (c) and (d) produce boundary conditions for the velocity perturbation \mathbf{v} , which, because of their symmetry, do not lead to torque. The torque on the particle has therefore the form $T_1 = a - b \cos 2\theta$.

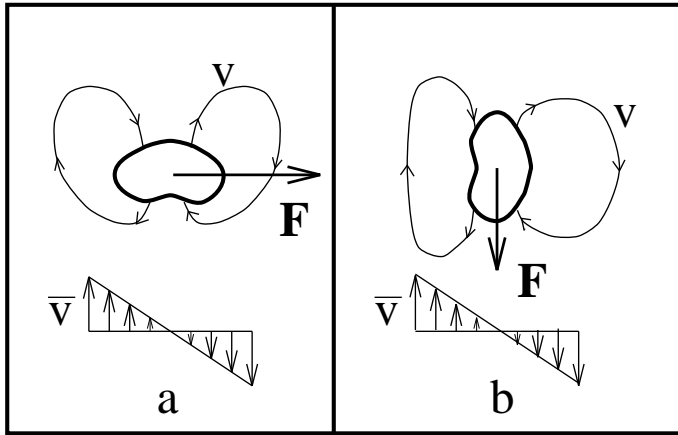


FIGURE 3. Forces on particles lacking fore-aft symmetry [see Eqns. (4.9) and (4.14)]. In case (a), top velocity lines (going towards the left) do not correspond to bottom ones (going to the right); the end result is a force in the horizontal direction. To each line going upwards, instead, there is a symmetric one going downwards (see e.g. portions of the velocity lines to the extreme left and extreme right of the particle). Hence, no vertical component in the velocity is present. Analogous reasoning show that in case (b), fore-aft asymmetry leads to a vertical force.

5. Shear induced diffusion of non-spherical particles

In the absence of external torques and forces, the far field behavior of the velocity perturbation around a particle, will be dominated by $l = 2$ scalar and electrical spherical harmonics, as it is clear from Eqn. (2.9a). As shown in Fig. 4, in the case of a spherical particle, this perturbed velocity will have the form of a quadrupole field with symmetry axes at 45° with respect to the flow direction (see Batchelor 1967). Due to this fact, if only binary particle-particle and particle-external obstacle interactions are taken into account, no transverse migration and diffusion processes can take place in creeping flow conditions. Thus, for spherical particles, transverse diffusion must be at least a second order process in the particle concentration (Leighton & Acrivos 1987). In Fig. 4, it is shown on the example of a large cross section encounter, how, due to symmetry, the total transverse displacement in a particle-particle encounter must necessarily be zero for a spherical particle. Because of the symmetry of the images and counterimages generated in the perturbed velocity field, by each sphere on the other one, it is easy to see that the result remains true also for close encounters. Detailed analysis of the hydrodynamic interaction of two spheres at arbitrary separations was carried on by Batchelor & Green (1972).

In Olla (1997a,b) it was shown that ellipsoidal particles, under certain conditions (in particular, deformability of the particle and closeness to a wall bounding the fluid) could migrate across flow lines. In the present section, it will be shown that, for a suspension of non-spherical particles, transverse diffusion is produced already thanks to binary inter-particle interactions, and there is a linear contribution in the concentration, to the transverse diffusivity. For the sake of simplicity, only contributions from large separation particle encounters are taken into consideration.

Because of symmetry, an $l = 2$ contribution to the velocity disturbance by the particle can be produced only if the particle shape is even (e.g. an ellipsoidal); for instance, the lowest vector spherical harmonics contributing to \mathbf{v} , produced by the $l = 3$ terms in Eqn. (4.1), will be $l = 3$ themselves. These will be negligible in the far field regime, compared to the quadrupole contributions from $X_{l=2}$. The symmetry breaking produced by these terms is what leads to the non-zero transverse particle displacement necessary for diffusion. Some of the necessary calculations are lengthy, but can easily be carried out with the help of a symbolic manipulation program like Maple.

To fix the ideas, consider a suspension of axisymmetric ellipsoids in a linear shear. Adopt a reference frame translating with one of the particles, and choose again the axes in such a way that the external flow can be written in the form: $\bar{\mathbf{v}} = \kappa \mathbf{e}_3 x_2$. Introduce again, also a primed reference frame with the x'_3 axis in the direction of the ellipsoid symmetry axis; the particle shape will be described, in this reference frame, by an equation in the form: $X(\mathbf{r})/r = 1 + \epsilon Y_{20}(\hat{x}'_i)$. The particle in exam will feel the passage of the others due to the velocity perturbation they produce in the fluid. For large separation encounters, the effect on the first particle can be calculated to lowest order in a perturbation series, in which corrections to the passing particles trajectories, due to the particle at the centre of the axes, are neglected. Likewise, no correction to the velocity perturbation in the fluid by the passing particles, due to the presence of the first one, is taken into account.

The velocity field that the first particle feels at time τ , as another particle passes by, is in the form: $\mathbf{u}(\theta_0, \phi_0, \tau - t, \mathbf{x}_\perp)$, where θ_0 and ϕ_0 are the angles giving the orientation of the symmetry axis of the passing particle at some reference time, t is the time the particle is at $x_3 = 0$. Due to the uniform translation of the particles, it is also possible to write: $\mathbf{u} = \mathbf{v}(\theta(\tau), \phi(\tau), \kappa x_2(\tau - t), \mathbf{x}_\perp)$, with $\mathbf{v}(\theta, \phi, x_3, \mathbf{x}_\perp)$ the orientation dependent velocity perturbation by the passing particle. A diffusion coefficient is obtained summing

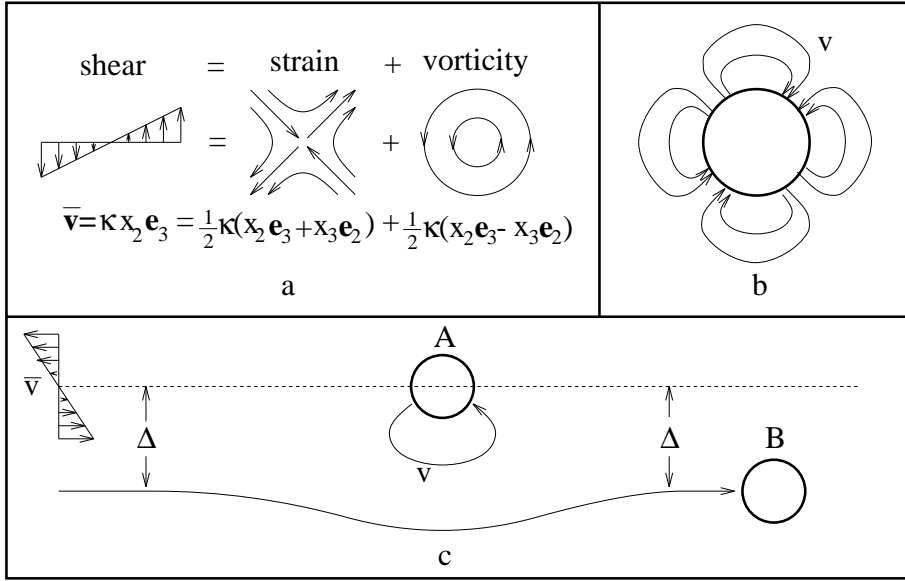


FIGURE 4. Encounter of two particles travelling with different velocity in a linear shear flow. See in (a) and (b) the decomposition of a linear shear in strain and vorticity part, and the kind of velocity perturbation produced around a spherical particle; due to the form of the Stokes equation, the same quadrupole symmetry of the strain is preserved in the velocity perturbation. This leads to the fact that a binary encounter produces no transverse displacement of the particles. Longitudinal displacements take instead place, moving the particles forward with respect to their unperturbed trajectories.

over the square displacement produced by the different particles in a time interval T ; restricting to contributions from particles at cross-separations greater than a certain x_{\perp} , one finds, for $\kappa T \rightarrow \infty$:

$$\begin{aligned}
 \mathbf{D}(x_{\perp}) &= T^{-1} \sum_i \Delta \mathbf{x}_i(T) \Delta \mathbf{x}_i(T) \\
 &= \frac{\rho \kappa}{T} \int_{-\infty}^{\infty} dt \int_{x_{\perp}}^{\infty} x_{\perp}^2 dx_{\perp} \int_0^{2\pi} d\psi \sin \psi \left| \int_0^T d\tau d\tau' \langle \mathbf{v}(\kappa x_2(\tau-t), \mathbf{x}_{\perp}) \mathbf{v}(\kappa x_2(\tau'-t), \mathbf{x}_{\perp}) \rangle \right| \\
 &= \rho \kappa \int_{x_{\perp}}^{\infty} x_{\perp}^2 dx_{\perp} \int_0^{2\pi} d\psi \sin \psi \langle \Delta \mathbf{x}(T) \Delta \mathbf{x}(T) \rangle + \mathcal{O}(T^{-1}) \quad (5.1)
 \end{aligned}$$

where $\Delta \mathbf{x}(T)$ is the particle displacement in a time T , ρ is the particle concentration, $x_2 = x_{\perp} \sin \psi$ and the averages are on the initial orientation $\{\theta_0 \phi_0\}$.

It is thus necessary from the start, in order to have a non-zero transverse diffusivity, that the transverse displacement $\Delta \mathbf{x}_{\perp}(T \rightarrow \infty)$ be itself non-zero. In the case of a sphere, from Eqn. (4.4), $\mathbf{v}_{\perp}^{(0)}$ is odd in x_3 and $\Delta \mathbf{x}_{\perp} = 0$ identically (see Fig. 4). Thus, the contribution from $\mathbf{v}^{(1)}$ must be taken into account. Notice that, again from Eqn. (4.4), for fixed x_{\perp} , inter-particle interactions are strong for $x_3 \sim x_{\perp}$, which means that the interaction time is, unless $\psi \simeq 0$, of the order of κ^{-1} . Since this is also the time-scale for particle rotation, no averaging away of the particle asymmetry takes place in an encounter time and a non-zero transverse displacement is expected.

From Eqns. (4.3-4), the coefficients in the expansion for $\mathbf{v}^{(1)}$ involve matrix elements in the form: $\langle \mu 2m | Y_{2m'} | \mathbf{v}' \rangle = \int d\Omega_x Y_{2m'} \mathbf{Y}_{2m}^{\mu*} \cdot \mathbf{v}'$, where, from Eqn. (4.4):

$$\mathbf{v}' = -\partial_r(\mathbf{v}^{(0)}(\mathbf{r}) + \bar{\mathbf{v}}(\mathbf{r})) = 10r^{-2} x_2 x_3 \kappa \mathbf{x} - 5\kappa[0, x_3, x_2] \quad (5.2)$$

The only non-zero matrix elements are the following:

$$\begin{cases} \langle e2-2|Y_{21}|\mathbf{v}'\rangle = \langle e22|Y_{2-1}|\mathbf{v}'\rangle = -\frac{25i}{128}\sqrt{6}\pi \\ \langle e2-1|Y_{20}|\mathbf{v}'\rangle = \langle e21|Y_{20}|\mathbf{v}'\rangle = \frac{175i}{128}\pi \\ \langle e2-1|Y_{22}|\mathbf{v}'\rangle = \langle e21|Y_{2-2}|\mathbf{v}'\rangle = -\frac{25i}{256}\sqrt{6}\pi \end{cases} \quad (5.3)$$

To obtain explicitly $\mathbf{v}^{(1)}$ it is necessary to write the non-sphericity components X_{lm} in the laboratory frame. Once the rotation matrix $d_{mm'}^{(2)}$ is known, one will have, on the surface $x = r$:

$$\mathbf{v}^{(1)}(\mathbf{r}) = \epsilon \sum_{mm'} d_{m'0}^{(2)} \langle e2m|Y_{2m'}|\mathbf{v}'\rangle \mathbf{Y}_{2m}^e(\hat{x}_i) \quad (5.4)$$

Now, from Eqn. (2.9a), one finds: $v_{e2m}^{(1)}(r) = -\sqrt{\frac{2}{3}}b_{2m}^{(1)}$ and then also: $a_{2m}^{(1)} = -b_{2m}^{(1)} = \sqrt{\frac{3}{2}}v_{e2m}^{(1)}(r)$. For large cross section encounters, it is enough to know the large distance asymptotic behavior of $\mathbf{v}^{(1)}$:

$$\mathbf{v}^{(1)}(\mathbf{x}) = \sum_m \sqrt{\frac{3}{2}}v_{e2m}^{(1)}(r)(r/x)^2 \mathbf{Y}_{2m}^s(\hat{x}_i) \quad (5.5)$$

The rotation matrix can be obtained using an adequate set of angles. If the deviation from spherical shape is small, the rotation of the particle will be, to lowest order, a uniform rotation around x_1 with angular velocity $\kappa/2$ (see Appendix). At some time, the x'_3 axis will lie in the x_1x_3 plane, forming an angle ϕ with x_3 . If one takes at that particular instant $x_2 = x'_2$, at a generic instant τ , the orientation of the particle will be given by a rotation of angle ϕ in the plane x_1x_3 , followed by another one by an angle θ in the plane x_2x_3 . From Eqn. (5.4), one needs the following terms from the rotation matrix:

$$\begin{cases} d_{\pm 20}^{(2)} = \frac{\sqrt{6}}{4}(\cos^2\phi(\cos^2\theta - 2) + 1 \mp \sin 2\phi \sin \theta) \\ d_{\pm 10}^{(2)} = \frac{\sqrt{6}}{4}(i \cos^2\phi \sin 2\theta \mp \sin 2\phi \cos \theta) \\ d_{00}^{(2)} = \frac{3}{2}\cos^2\phi \cos^2\theta - \frac{1}{2} \end{cases} \quad (5.6)$$

Using Eqns. (5.3-4) and (5.6), one obtains for $v^{(1)}(\mathbf{r})$:

$$\begin{cases} v_{e20}^{(1)}(r) = 0 \\ v_{e2\pm 1}^{(1)}(r) = \frac{75\pi}{256} \left(i \left(\frac{17}{6} - \cos^2\phi \left(\frac{13}{2} \cos^2\theta + 1 \right) \right) \mp \sin 2\phi \sin \theta \right) \\ v_{e2\pm 2}^{(1)}(r) = \frac{75\pi}{256} \left(-\cos^2\phi \sin 2\theta \pm i \sin 2\phi \cos 2\theta \right) \end{cases} \quad (5.7)$$

From here, it is possible to obtain the displacement from a binary encounter. For a large cross section encounter, the asymptotic expression for $\mathbf{v}^{(1)}(\mathbf{x})$, provided by Eqn. (5.5), is sufficient. Remembering that $x_3 = \kappa x_2(\tau - t)$, $\theta(t) = \theta_0 + \frac{\kappa\tau}{2}$, $\phi(t) = \phi_0$ and using standard expressions for the $l = 2$ spherical harmonics in Eqn. (5.5): $Y_{2\pm 1} = \sqrt{\frac{15}{8\pi}} \frac{x_3(-ix_2 \mp x_1)}{x^2}$ and $Y_{2\pm 2} = \sqrt{\frac{15}{2\pi}} \frac{x_1^2 - x_2^2 \pm ix_1x_2}{4x^2}$, one finds therefore:

$$\Delta\mathbf{x}_\perp = \int_{-\infty}^{\infty} d\tau \mathbf{v}_\perp^{(1)}(\theta(\tau), \phi(\tau), \mathbf{x}(\tau)) = \frac{225\sqrt{5\pi}}{1024} \frac{r^3}{x_\perp^2} G(\theta_0, \phi_0, \psi) (\cos \psi \mathbf{e}_1 + \sin \psi \mathbf{e}_2) \quad (5.8)$$

where

$$\begin{aligned} G(\theta_0, \phi_0, \psi) = & \cos^2\phi_0 \sin 2\theta_0 \left(\frac{13}{2} \sin \psi F_1(\sin \psi) - \cos 2\psi F_0(\sin \psi) \right) \\ & + 2 \sin 2\phi_0 \cos \theta_0 \left(\cos \psi F_1(2 \sin \psi) - \sin 2\psi F_0(2 \sin \psi) \right) \end{aligned} \quad (5.9)$$

The functions F_i involve Bessel functions and originate from integrals in the form $\int dt \frac{\cos \gamma t}{(1+t^2)^{5/2}}$ and $\int dt \frac{t \sin \gamma t}{(1+t^2)^{5/2}}$ arising in Eqn. (5.9) (Gradshteyn & Ryzhik 1965). Their explicit form is:

$$\begin{cases} F_0(\gamma^{-1}) = 2(\gamma^2 K_0(\gamma) + \gamma K_1(\gamma)) \\ F_1(\gamma^{-1}) = 2(-\gamma K_0(\gamma) + \gamma^2 K_1(\gamma)) \end{cases} \quad (5.10)$$

with K_i modified Bessel functions of the second kind (Abramowitz & Stegun 1965). Substituting Eqns. (5.8-10) into Eqn. (5.1), it is possible to carry out the integrals over x_\perp , θ_0 and ϕ_0 analytically, and the remaining one in ψ numerically. The final result for the contribution to the transverse diffusivity from particle encounters at cross separation greater than x_\perp is:

$$\mathbf{D}(x_\perp) \simeq (2.85\mathbf{e}_1\mathbf{e}_1 + 5.99\mathbf{e}_2\mathbf{e}_2) \frac{\rho\kappa r^6}{x_\perp} \quad (5.11)$$

Of course the bulk of the diffusivity is produced by close particle encounters and the present analysis can give at most an estimate, or some kind of lower bound for this quantity.

It is interesting to compare Eqn. (5.11) with analogous results for longitudinal shear induced diffusion in suspensions (Acrivos *et al.* 1992). In that case, there was a singular contribution coming from encounters between particles lying in the same x_1x_3 plane. The source of the singularity lied in the long interaction time of particles travelling essentially with identical speed. In the present case, this divergence is cured by the averaging out of the particle asymmetry effect, produced by the many rotations that a particle would carry out during an encounter at $x_2 \simeq 0$.

The basic result of this section is that binary inter-particle interactions contribute to transverse diffusion in a suspension of non-spherical particles. An additional mechanism for the generation of diffusive behaviors has recently been suggested (Stone 1997), based on the possibility of chaos in the orientation angles dynamics, in the absence of particle encounters. This would imply a contribution to diffusion which would be concentration independent and would become important in the case of dilute suspensions. This mechanism becomes easy to understand going back to the situation considered in section IV. It was shown there, that particles with no fore-aft symmetry, immersed in linear shear flows, carried on a kind of motion, which involved translation of their centre of mass, and which depended on the particle orientation. This means an evolution equation for the centre of mass coordinate in the form $\dot{\mathbf{x}}_{CM} = \mathbf{u}_{CM}(\theta_i)$, with θ_i the angles giving the orientation of the particle. Already on an intuitive basis, only a chaotic behavior of θ_i , with orbits of arbitrarily long period, would guarantee the presence of the low frequency components in the \mathbf{u}_{CM} spectrum, necessary for the divergence at large t , of $\langle |x_{CM}(t) - x_{CM}(0)|^2 \rangle$.

The possibility of chaos for θ_i arises in the case of non axisymmetric particles, from the fact that three angles θ_i are required to fix the orientation, and from the non-linear character of the equations describing their evolution. (Chaos, of course, would be excluded in the case of axisymmetric particles, for which only two angles are necessary to fix orientation). This situation is in some sense analogous to the one of the asymmetric rigid body. For small deviations from spherical shape (small ϵ), however, analysis carried out in the Appendix suggests that chaotic behaviors, if present, take place at very long time scales $\epsilon^{-2}\kappa^{-1}$, which are irrelevant for the problem in exam.

6. Torque on non fore-aft symmetric particles in quadratic shear flows

One of the reasons why this problem is of practical relevance, is to understand the mechanism of particle migration towards the middle of channel and pipe flows, when the particle size and that of the channel gap (or pipe diameter) become comparable (see Helmy & Barthes-Biesel 1982, Leyrat & Barthes-Biesel 1994 and Couillette & Pozrikidis 1998). Nadim & Stone (1991) calculated analytically the velocity field around a droplet, together with its deformations, in a quadratic shear flow. However, the modifications in the droplet dynamics, produced by the $l = 3$, quadratic shear produced part of the deformation, were left out of their treatment.

In haemodynamics, the migration of red cells towards the middle of small blood vessels, is a well known phenomenon, which has the name of Fahraeus-Lindqvist effect (Oiknine 1976). It has been shown (see Olla 1997a,b), that even neglecting inertial forces, ellipsoidal particles migrate away or towards the closest channel boundary depending on their instantaneous orientation. More precisely, particles migrate towards the wall if their longer axis is aligned with the stretching direction of the strain, and away from it when this axis is aligned with the compressing direction. Unfortunately, given the form of the angular velocity for such ellipsoidal particles, which is given by Jeffery's expression $\omega = a - b \cos 2\theta$, with θ the angle between the ellipsoid major axis and the flow direction, the particle will spend equal time in both orientation and no average drift is possible. As it is shown in Fig. 5, inclusion of quadratic contributions to shear, does not change the situation, if the particle shape remains fore-aft symmetric. It turns out that the simplest way the odd contribution to torque, necessary to break the symmetry between the two particle orientations, is to consider at the same time fore-aft violating particle shapes and the quadratic contribution to shear. In fact, breaking fore-aft symmetry, is not enough to produce odd contribution to torque if the shear is purely linear (see Fig. 6).

Consider a particle in a channel flow, which, in a reference frame centred at the particle and translating with it, reads: $\bar{\mathbf{v}} = [0, 0, \kappa(r^2/3 - x_2^2)]$. Hence, from Eqn. (3.9), no external forces are necessary to maintain this particle in its state of motion. Take the particle shape to be described in a reference frame $\{x'_1 x'_2 x'_3\}$, by the equation $X'(\hat{x}'_i)/r = 1 + \epsilon Y_{30}(\hat{x}'_i)$; thus the particle is axisymmetric with symmetry axis along x'_3 . Take this symmetry axis to lie in the $x_2 x_3$ plane, at an angle θ with x_3 (see Fig. 5). It is easy to see that the form of the functional dependence on θ , of the torque on this particle, must be necessarily in the form $T_1 = \sin \theta(a - b \cos^2 \theta)$, independently of deviations from spherical shape. Setting $x'_1 = x_1$ in the primed reference frame, so that x'_2 lies in the $x_2 x_3$ plane, the velocity of the particle surface can be written as follows:

$$\begin{aligned} & \mathbf{e}'_2 x'_2 \sin \theta \cos^2 \theta + \mathbf{e}'_2 x'_3 \sin^3 \theta - 2\mathbf{e}'_3 x'_2 x'_3 \cos^2 \theta \sin \theta \\ & - 2\mathbf{e}'_2 x'_2 x'_3 \sin^2 \theta \cos \theta + \mathbf{e}'_3 x'_2 \cos^3 \theta + \mathbf{e}'_3 x'_3 \cos \theta \sin^2 \theta \end{aligned} \quad (6.1)$$

To calculate the torque on a spheroidal particle, it is necessary to know the $\mathcal{O}(\epsilon)$ term $\mathbf{v}^{(1)}$ in the velocity perturbation. By symmetry only the torque T_1 is non-zero: $T_1 = \langle T_1 | \mathbf{v}^{(1)} \rangle$. In order to calculate $\mathbf{v}^{(1)}$, from Eqn. (4.3), it is necessary first to know the components of $\mathbf{v}^{(0)}$, which are obtained from those of $\bar{\mathbf{v}}$, simply by a change of sign. Expanding $\mathbf{v}^{(0)}$ and $\bar{\mathbf{v}}$, using respectively Eqns. (2.9a) and (2.9b), it is possible to write for $\mathbf{v}' = -\partial_r(\bar{\mathbf{v}} + \mathbf{v}^{(0)})|_{x=r}$:

$$\mathbf{v}' = \sum_{\mu lm} v'_{\mu lm} \mathbf{Y}_{lm}^{\mu} = \sum_{lm} (2l+1) \left[\left(-\frac{3}{\sqrt{l(l+1)}} \bar{v}_{slm} + 2\bar{v}_{elm} \right) \mathbf{Y}_{lm}^e + \bar{v}_{mlm} \mathbf{Y}_{lm}^m \right] \quad (6.2)$$

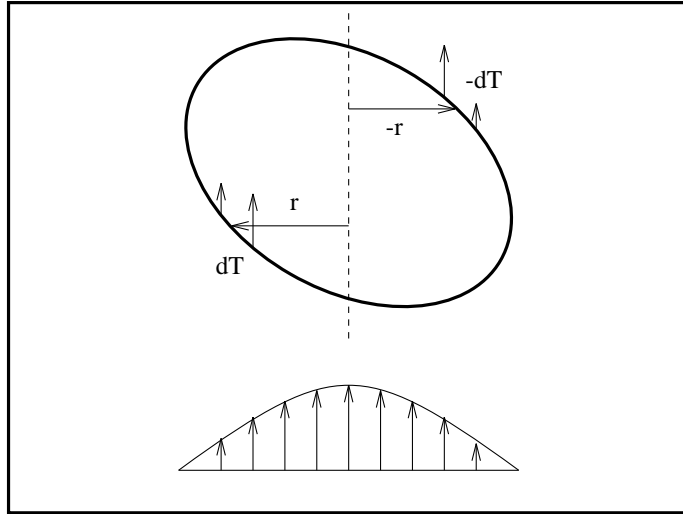


FIGURE 5. Fore-aft symmetric particle in quadratic shear: no torques are produced. Because of symmetry of both the particle shape and the velocity field, for any surface element at \mathbf{r} , there is another one at $-\mathbf{r}$, such that the contributions to torque are equal and opposite.

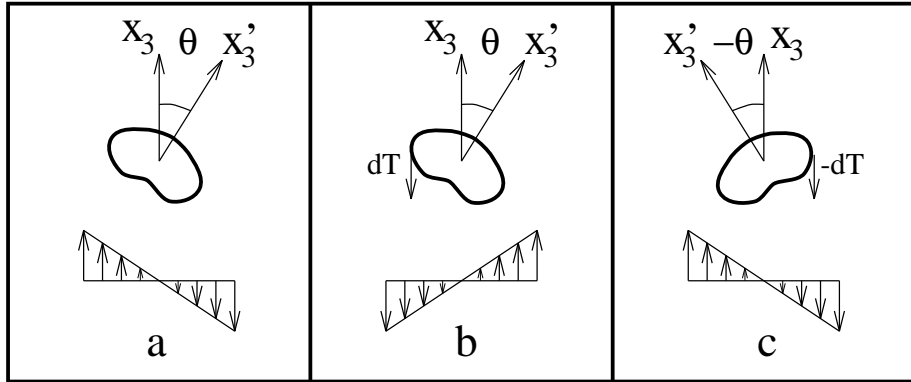


FIGURE 6. The torque on a fore-aft asymmetric particle in a linear shear, does not contain odd θ contributions. Case (b) is obtained from case (a) changing sign to the velocity at all points on the particle surface. Hence the torques in (a) and (b) are equal and opposite. Case (c) is obtained from (b) by a reflection. The velocity, and therefore also the force, remain the same, point by point on the particle surface. The position vector from x_3 to the point on the surface, however changes sign, and then the torque is the opposite to that in case (b). Hence the torque in (a) and in (c) are equal.

The non-zero components of $\bar{v}_{\mu lm}$ are easily calculated with the help of Maple:

$$\left\{ \begin{array}{l} \bar{v}_{s10} = \kappa r^2 \frac{4\sqrt{3\pi}}{45}; \quad \bar{v}_{s30} = \kappa r^2 \frac{2\sqrt{7\pi}}{35}; \quad \bar{v}_{s32} = \bar{v}_{s3-2} = \kappa r^2 \frac{\sqrt{210\pi}}{105}; \\ \bar{v}_{e10} = -\kappa r^2 \frac{2\sqrt{6\pi}}{45}; \quad \bar{v}_{e30} = \kappa r^2 \frac{4\sqrt{21\pi}}{105}; \quad \bar{v}_{e32} = \bar{v}_{e3-2} = \kappa r^2 \frac{2\sqrt{70\pi}}{105} \\ \bar{v}_{m22} = -\bar{v}_{m2-2} = \kappa r^2 \frac{2i\sqrt{5\pi}}{15} \end{array} \right. \quad (6.3)$$

Using Eqn. (4.11) to obtain the expression for X in the laboratory frame, and Eqn. (4.3)

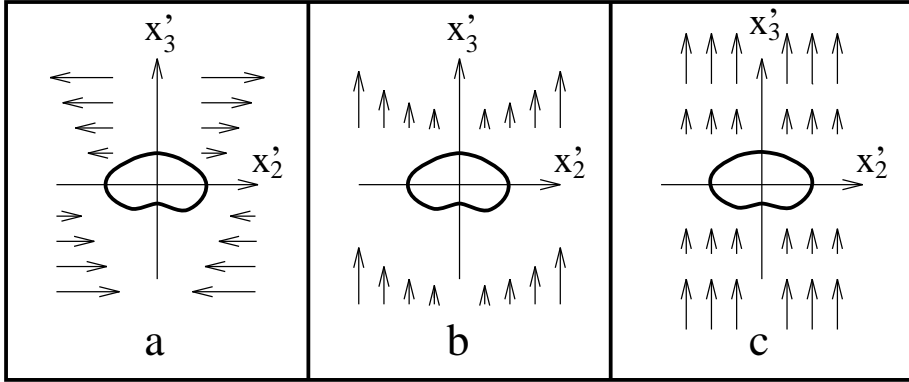


FIGURE 7. Terms in the decomposition of a quadratic shear in terms of primed variables, which do not contribute to torque. Flows (a-c) correspond to the terms on the second line of Eqn. (6.1)

to express $\mathbf{v}^{(1)}$ in function of \mathbf{v}' , it is possible to write:

$$T_1 = \epsilon \sum_{\mu l m m'} \langle T_1 | Y_{3m'} | \mu l m \rangle v'_{\mu l m} d_{0m'}^{(3)} \quad (6.4)$$

The matrix $\langle T_1 | Y_{3m'} | \mu l m \rangle$ can be obtained again with the help of Maple, and its non-zero entries are given for reference below:

$$\left\{ \begin{array}{l} \langle T_1 | Y_{31} | e10 \rangle = \langle T_1 | Y_{3-1} | e10 \rangle = \frac{9i\pi\sqrt{14}}{256} \mu r^2 \\ \langle T_1 | Y_{31} | e32 \rangle = \langle T_1 | Y_{3-1} | e3-2 \rangle = \frac{273i\pi\sqrt{30}}{2048} \mu r^2 \\ \langle T_1 | Y_{33} | e32 \rangle = \langle T_1 | Y_{3-3} | e3-2 \rangle = \frac{525i\pi\sqrt{2}}{2048} \mu r^2 \\ \langle T_1 | Y_{31} | m22 \rangle = -\langle T_1 | Y_{3-1} | m2-2 \rangle = -\frac{15\pi\sqrt{105}}{512} \mu r^2 \\ \langle T_1 | Y_{33} | m22 \rangle = -\langle T_1 | Y_{3-3} | m2-2 \rangle = -\frac{75\pi\sqrt{7}}{512} \mu r^2 \end{array} \right. \quad (6.5)$$

Substituting this, together with Eqns. (6.2-3) and (4.14), into Eqn. (6.4), the following expression for the torque is obtained:

$$T_1 = -\kappa\mu r^4 \left(\frac{1617}{10240} + \frac{933}{2048} \cos^2 \theta \right) 7^{\frac{1}{2}} \pi^{\frac{3}{2}} \sin \theta \quad (6.6)$$

which indicates that there is only one stable orientation of the particle: $\theta = 0$, corresponding to the particle fore being aligned in the direction of the flow.

7. Conclusions

The work presented in this paper has been carried on along two parallel lines: the derivation of qualitative results on the behavior on particles in shear flows, by means of simple geometrical reasoning, and actual quantitative calculations, using perturbation theory around the case of a spherical particle. Emphasis was put, especially in the geometrical proofs, on the origin of the results, in the symmetries of Stokes dynamics. In the quantitative calculations, this had its counterpart, in the power of methods based on the use of vector spherical harmonics.

Of course, a vector spherical harmonics representation is equivalent to one based on the use of irreducible tensors, and the second has been used extensively (see e.g. Nadim & Stone 1991, Happel & Brenner 1965). Vector spherical harmonics, however, seem more compact and the identification of pressure terms, potential terms and pressure free vortical terms [the $a - c$ coefficients in Eqn. (2.9a-b)] is physically meaningful.

In the case of spherical particles, these methods allowed direct calculation of torques and forces, without any need of informations on the velocity perturbation produced by the particle. This, independently of the form of the external velocity field and of possible tangential streaming behaviors of the particle surface. In this respect, the present method is equivalent to the one presented in Stone (1997), based on use of the reciprocity theorem (Happel & Brenner 1965). The power of the method becomes apparent in perturbation theory, since it allows to see more clearly how different symmetries in the particle shape and in the external flow, couple together to produce velocity perturbations around the particle and modifications to its trajectory. In particular, it has been possible to show that only certain shapes can lead to force and torques. In linear shears, only $l = 2$ and $l = 3$ deviations from spherical shape, respectively, lead to torques and forces acting on the particle. For large deviations from spherical shape, the statement ceases to refer to spherical harmonics components of the particle shape, and shifts to the fore-aft symmetry of this shape.

The techniques presented have been applied to the analysis of two important problems: the calculation of the transverse displacement, resulting from a large cross section encounter between two ellipsoidal particles in a Couette flow, and the torque on a particle whose shape is not fore-aft symmetric, produced by quadratic components in the shear. It has thus been possible, to calculate the contribution to transverse diffusion from large cross section two-particle interactions, leading to the expression for diffusivity in the dilute suspension limit: $D \sim \rho \kappa r^5$ with ρ the particle density, κ the shear rate and r the particle size. The question of self-diffusion of individual particle trajectories remains instead open. The present analysis shows that this effect could become important only for large deviations of the particle shape from spherical. Numerical solution of Jeffery's equations (Jeffery 1922), to search for chaotic solutions, and stability analysis of the steady rotation solutions presented in that paper, could be an interesting approach to the problem.

The analysis of the behavior of a spheroidal particle in a channel flow, apart of the simple result on the force on a spherical particle at the centre of the channel, has allowed to calculate the torque forcing a particle lacking fore-aft symmetry, to align its fore in the direction of the flow. Olla (1998) showed recently that violation of fore-aft symmetry, is a necessary condition for the fast migration of red cells towards the middle of small blood vessels (Fahraeus-Lindqvist effect, see Oiknine 1976) exactly because of this torque.

As a final remark, knowledge of the velocity perturbation produced by particles of different shapes in different fluid flows, is one of the necessary elements to write codes for the simulation of suspension dynamics, based on the use of particle methods (see Bossis & Brady 1984). Such codes by-pass the calculation of the flow velocity at all points in the fluid, by treating the particle dynamics in terms of effective interactions. It would be interesting to understand how, inclusion of the kind of effects considered in the present paper, would modify the macroscopic behaviors resulting from such simulations.

I would like to thank Howard Stone for many suggestions, and for interesting and helpful conversation. Part of this research was carried on at CRS4 and at the Laboratoire de Modélisation en Mécanique in Jussieu. I would like to thank Gianluigi Zanetti and Stephane Zaleski for hospitality.

Appendix A. The possibility of self-diffusion

Self-diffusion of particle trajectories becomes a possibility when the evolution of the particle orientation angles is chaotic. In fact, if the particle is not fore-aft symmetric,

there will be angle dependent forces, leading to a time dependent drift, that, for small deviations from spherical shapes, will be in the form:

$$\Delta \dot{x}_i(t) = F_i^{lm} X_{lm}(t) \quad (A1)$$

(Summation over repeated indices is understood in the present appendix). In Eqn. (A1), the drift matrix F_i^{lm} gives the velocity with which the particle moves under the effect of the force $R^F X$ [see Eqn. (4.5)]. If the deviation from sphericity: X_{lm} $l > 0$, is not small, the drift matrix will itself be dependent upon $X_{lm}(t)$, i.e. upon orientation. Self diffusion arises if the limit for $t \rightarrow \infty$ of $D(t) = t^{-1} \langle |\Delta \mathbf{x}(t)|^2 \rangle$ is non-zero. In such a case, from Eqn. (A1), it would be possible to write:

$$D(\infty) = \int_0^\infty dt \langle \Delta \dot{x}^i(t) \Delta \dot{x}_i(0) \rangle = F_i^{lm} F^{il'm'} \int_0^\infty dt \langle X_{lm}(t) X_{l'm'}(0) \rangle. \quad (A2)$$

It is then necessary that the variables $X_{lm}(t)$ became uncorrelated at sufficiently large time separations. In the case of a chaotic system, the correlation $\langle X_{lm}(t) X_{l'm'}(0) \rangle$ would have an oscillatory component, but, at times large compared to the Lyapunov time, the oscillations would be damped away and the correlation would go to zero.

Dynamical equations for the orientation can be obtained starting from the angular velocity; assuming an external flow in the form $\bar{\mathbf{v}} = (\kappa/2) \mathbf{e}_3 x_2$:

$$\omega_i = \frac{\kappa}{2} \delta_i^1 + M_i^{lm} X_{lm} \quad (A3)$$

where the matrix M gives the contribution to angular velocity coming from the torque R^T , in the same way as F , in Eqn. (A1), gave the translation velocity coming from the force R^F . The rotation of the particle will thus be described by the equation:

$$\dot{X}_{lm} = \omega_i L_{lm}^{il'm'} X_{l'm'} = \frac{\kappa}{2} L_{lm}^{1l'm'} X_{lm} + M_{ilm}^{l'm'} L_{lm}^{il''m''} X_{l'm'} X_{l''m''} \quad (A4)$$

where the matrix L is the generator of the rotations in the group representation provided by the X_{lm} . (Albeit constant factors, the terms $L_{lm}^{1l'm'}$ are basically the matrix elements of the quantum mechanical angular momentum operator \mathbf{L} with respect to the states $|lm\rangle$ and $|l'm'\rangle$).

In the reference frame rotating around x_1 with angular velocity $\omega^{(0)} = \kappa/2$, Eqn. (A4) will read:

$$\dot{X}'_{lm} = \omega'_i L_{lm}^{il'm'} X'_{l'm'} \quad (A5)$$

where $X'_{l'm'} = d_{lm}^{l'm'} X_{l'm'}$, with $d_{lm}^{l'm'} \equiv \delta_l^l d_{mm'}^{(1)}$ the rotation matrix relating X in the rotating and laboratory reference frames. Indicating with U , the rotation matrix for vectors, the angular velocity ω' will read, from Eqns. (A3) and (A5):

$$\omega'_i = U_i^j M_j^{l'm'} \tilde{d}_{l'm'}^{l''m''} X_{l''m''} \quad (A6)$$

with \tilde{d} the inverse of d . The final equation for $X'_{lm}(t)$ is then:

$$\dot{X}'_{lm} = U_i^j \tilde{d}_{l'm'}^{l''m''} M_j^{l'm'} X'_{l''m''} X'_{l'''m'''}. \quad (A7)$$

This equation is in the form $\dot{x}(t) = \epsilon a(t)x(t)x(t)$, with ϵ small, giving essentially the degree of non-sphericity of the particle shape, and $a(t)$ varying on a $\mathcal{O}(1)$ time scale. This equation can thus be solved by multiple scale expansion:

$$\dot{X}'_{lm} = \langle U_i^j \tilde{d}_{l'm'}^{l''m''} \rangle M_j^{l'm'} X'_{l''m''} X'_{l'''m'''}. \quad (A8)$$

Unfortunately, in the case of Eqn. (A7), the only non-zero contribution in the average

corresponds to a component along x_1 of the angular velocity ω' (no alternative preferential directions are present in the product $U_i^j \tilde{d}_{l'm''}^{l''m''''}$). Thus, the dynamics of Eqn. (8) is essentially one-dimensional and no chaos can arise to this order in perturbation theory.

This has two consequence. First, secular terms lead to a change in the rotational motion of the particle in a time that is at least ϵ^{-2} longer than the rotation period. Hence, approximating the particle motion with a steady rotation, was perfectly adequate for the analysis of binary particle interactions carried out in section V. Second, the self-diffusivity D is expected to be at least $\mathcal{O}(\epsilon^6)$. In fact, Eqn. (A2) can be re-written in terms of primed variables:

$$D(\infty) = F_i^{lm} F^{il'm'} \int_0^\infty dt d_{lm}^{l''m''} \langle X_{l'm''}^l(t) X_{l'm'}^l(0) \rangle. \quad (A9)$$

and the integral can be seen as a Fourier transform at the rotation frequency of the particle, with $d_{l'm'}^{lm}$ the oscillating term, of a correlation function decaying at a time scale ϵ^{-2} longer. For an exponential decay, this implies that the integral is $\mathcal{O}(\epsilon^4)$, while each factor F_{lm} brings an additional factor ϵ .

REFERENCES

- M. ABRAMOWITZ AND I.A. STEGUN *Handbook of Mathematical Formulas* (Dover, New York, 1965)
- A. ACRIVOS, G.K. BATCHELOR, E.J. HINCH, D.L. KOCH AND R. MAURI 1992 Longitudinal shear induced diffusion of spheres in a dilute suspension. *J. Fluid Mech.* **20**, 651
- G.K. BATCHELOR 1967 *An Introduction to Fluid Mechanics* Cambridge University Press
- G.K. BATCHELOR AND J.T. GREEN 1972 The hydrodynamic interaction of two freely-moving spheres in a linear flow field. *J. Fluid Mech.* **56**, 375
- G. BOSSIS AND J. BRADY 1984 Dynamic simulation of sheared suspensions. *J. Chem. Phys.* **80**, 5141
- C. COULLIETTE & C. POZRIKIDIS 1998, 1998 Motion of an array of drops through a cylindrical tube. *J. Fluid Mech.* **258**, 1
- B.U. FELDERHOF AND R.B. JONES 1994a Inertial effects in small-amplitude swimming of a finite body. *Physica A* **202**, 94
- B.U. FELDERHOF AND R.B. JONES 1994b Small amplitude swimming of a sphere. *Physica A* **202**, 119
- I.S. GRADSHTEYN AND I.M. RYZHIK 1965 *Tables of Integrals, Series and Products* Academic Press, New York
- J. HAPPEL & H. BRENNER 1965, *Low Reynolds Number Hydrodynamics* Prentice-Hall
- A. HELMY & D. BARTHES-BIESEL 1982 Migration of a spherical capsule freely suspended in an unbounded parabolic flow. *J. Méc. Théor. Appl.* **1**, 859
- B.P. HO AND L.G. LEAL 1974 Inertial migration of rigid spheres in two-dimensional unidirectional flows. *J. Fluid Mech.* **65**, 365
- G.B. JEFFERY 1922 The motion of ellipsoidal particles immersed in a viscous fluid *Proc. R. Soc. Lond. A*, **102**, 161
- H. LAMB 1932, *Hydrodynamics* Cambridge University Press
- L.D. LANDAU & E.M. LIFSHITZ 1965, *Quantum Mechanics: Non-Relativistic Theory*, Pergamon Press
- L.D. LANDAU & E.M. LIFSHITZ 1982, *Quantum Electrodynamics*, Pergamon Press
- D. LEIGHTON & A. ACRIVOS 1987 The shear-induced migration of particles in concentrated suspensions *J. Fluid Mech.* **181**, 415
- A. LEYRAT & D. BARTHES-BIESEL 1994 Motion of a deformable capsule through a hyperbolic constriction *J. Fluid Mech.* **279**, 135

- J.B. MC LAUGHLIN 1993 The lift on small sphere in a wall-bounded linear shear flow *J. Fluid Mech.* **246**, 249
- A. NADIM & H.A. STONE 1991 The motion of small particles and droplets in quadratic flows. *Studies in Applied Mathematics* **85**, 53
- F. AZELVADRE AND C. OIKNINE 1976 Effect Fahraeus et effect Fahraeus-Lindqvist: Resultats experimentaux et models theoretiques *Biorheology* **13**, 315
- P. OLLA 1997a The role of tank-treading motions in the transverse migration of a spheroidal particle in a shear flow. *J. Phys. A (Math. Gen.)* **30**, 317
- P. OLLA 1997b The lift on a tank-treading ellipsoidal cell in a shear flow. *J. Phys. II (France)* **7**, 153
- P. OLLA 1998 A simplified model for red cell dynamics in small blood vessels. Submitted to *Phys. Rev. Lett.*
- W.B. RUSSEL, E.J. HINCH, L.G. LEAL & G. TIEFFENBRUCK 1977 Rods falling near a vertical wall. *J. Fluid Mech.* **83**, 27 3
- P.G. SAFFMANN 1964 The lift on a small sphere in a slow shear flow. *J. Fluid Mech.* **22**, 385
- H.A. STONE & A.D.T. SAMUEL 1996 Propulsion of microorganisms by surface distorsions. *Phys. Rev. Lett.* **77**, 4102
- H.A. STONE 1997, Private Communication
- P. VASSEUR AND R.G. COX 1976 The lateral migration of a spherical particle in two-dimensional shear flows *J. Fluid Mech.* **78**, 385